Study of a Bidirectional DC/DC Converter in Low Voltage Dual Powering Mode for EV Applications

Neha Gaikwad[1], Prof. Pawan C.Tapre[2]
[1]PG Student, [2]Assistant Professor
Department of Electrical Engineering
S.N.D.College of Engineering & Research Centre, Yeola
Savitribai Phule Pune University, Pune

Abstract- In this review paper, a study had been presented for a newly designed, patented, bidirectional dc/dc converter (BDC) that interfaces main energy storage (ES1), auxiliary energy storage (ES2), and dc-bus of different voltage levels, for application in hybrid electric vehicle systems. The proposed converter can operate in a step-up mode (i.e., low-voltage dual-source-powering mode) and a step-down (i.e., high-voltage dc-link energy-regenerating mode), both with bidirectional power flow control. In addition, the model can independently control power flow between any two low-voltage sources (i.e., low-voltage dual-source buck/boost mode). Herein, the circuit configuration, operation, relationships for steady-state analysis of the proposed BDC is discussed according to its three modes of power transfer.

Keywords- bidirectional converter, dual storage, electric vehicle, operating modes

I. INTRODUCTION

Global climate change and energy supply is declining have stimulated changes in vehicular technology. Advanced technologies are currently being researched for application in future vehicles. Among such applications, fuel-cell hybrid electric vehicles (FCV/HEV) are efficient and promising candidates. In the past, Ehsani et al. studied the vehicles' dynamics to look for an optimal torque-speed profile of the electric propulsion system [1]. Emadi et al. discussed the operating properties of the topologies for different vehicles including HEV, FCV, and more electric vehicles [2]. Emadi et al. also integrated power electronics intensive solutions in advanced vehicular power system to satisfy huge vehicular load [3]. Schaltz et al. sufficiently divide the load power among the fuel cell stack, the battery, and the ultra capacitors based on two proposed energy-management strategies [4]. Thounthong et al. studied the influence of fuel-cell (FC) performance and the advantages of hybridization for control strategies [5]. Chan et al. reviewed electric, hybrid, and fuel-cell vehicles and focused on architectures and modeling for energy management [6]. Khaligh and Li presented energy-storage topologies for HEVs and plug-in HEVs (PHEVs). They also discussed and compared battery, UC, and FC technologies. Furthermore, they also addressed various hybrid ESSs that integrate two or more storage devices [7]. Rajashekara reviewed the current status and the requirements of primary electric propulsion components-the battery, the electric motors, and the power electronics system [8]. Lai et al. implemented a bidirectional dc/dc converter topology with two-phase and interleaved characteristics. For EV and dc-microgrid systems, the converter has an improved voltage conversion ratio [9]. Furthermore, Lai also studied a bidirectional dc to dc converter (BDC) topology which has a high voltage conversion ratio for EV batteries connected to a dc-microgrid system [10]. In FCV systems, the main battery storage device is commonly used to start the FC and to supply power to the propulsion motor [2, 3]. The battery storage devices improve the inherently slow response time for the FC stack through supplying peak power during accelerating the vehicle [7]. Moreover, it contains a high power-density component such as super capacitors (SCs) eliminate peak power transients during accelerating and regenerative braking [11]. In general, SCs can store regenerative energy during deceleration and release it during acceleration, thereby supplying additional power. The high power density of SCs prolongs the life span of both FC stack and battery storage devices and enhances the overall efficiency of FCV systems [2-8, 12].

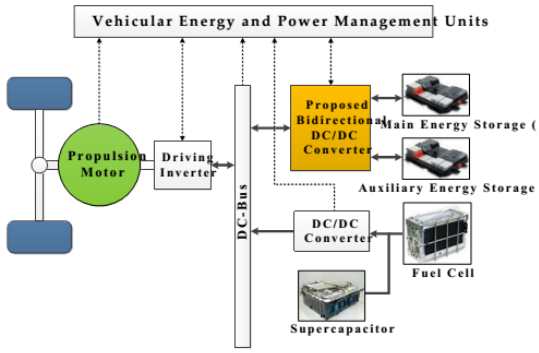

Fig.1: Functional diagram for a FCV/HEV power system.

The function of the bidirectional dc/dc converter (BDC) is to interface dual-battery energy storage with the dc-bus of the driving inverter. The study proposes a new BDC topology for FCV/HEV power systems that consists of an interleaved

voltage-doublers structure [9, 28] and a synchronous buck-boost circuit. It features two main operating modes: a low-voltage dual-source-powering mode and a high-voltage dc-bus energy-regenerating mode. In addition, the proposed converter can independently control power flow between any two low-voltage sources when in the low-voltage dual-source buck/boost mode. A similar topology was introduced in [28] that only describe a brief concept. By contrast, this study presents a detailed analysis of the operation and closed-loop control of this new topology as well as simulation and experimental results for all its modes of operation. Moreover, this study expanded the topology presented in [28] because the proposed converter can operate over a wider range of voltage levels. The main characteristics of the proposed converter are summarized as follows: 1) interfaces more than two dc sources for different voltage levels, 2) controls power flow between the dc bus and the two low-voltage sources and also independently controls power flow between the two low-voltage sources, 3) enhances static voltage gain and thus reduces switch voltage stress, and 4) possesses a reasonable duty cycle and produces a wide voltage difference between its high- and low-side ports.

II. PROPOSED METHODOLOGY

The proposed BDC topology with dual-battery energy storage is illustrated in Fig. 2, where V_H, V_{ES1}, and V_{ES2} represent the high-voltage dc-bus voltage, the main energy storage (ES1), and the auxiliary energy storage (ES2) of the system, respectively. Two bidirectional power switches (S_{ES1} and S_{ES2}) in the converter structure, are used to switch on or switch off the current loops of ES1 and ES2, respectively. A charge-pump capacitor (CB) is integrated as a voltage divider with four active switches (Q1, Q2, Q3, Q4) and two phase inductors (L1, L2) to improve the static voltage gain between the two low-voltage dual sources (VES1, VES2) and the high-voltage dc bus (VH) in the proposed converter. Furthermore, the additional CB reduces the switch voltage stress of active switches and eliminates the need to operate at an extreme duty ratio. This bidirectional power switch is implemented via two metal-oxide-semiconductor field-effect transistors (MOSFETs), pointing in opposite directions, in series connection.

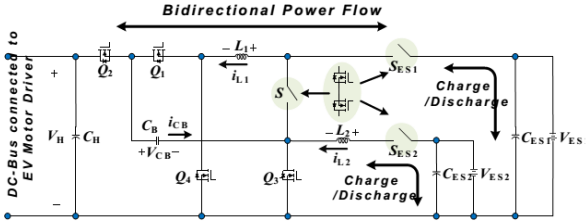

Fig.2: Proposed BDC topology with dual-battery energy storage.

TABLE I: OPERATING MODES OF BIDRECTIONAL DC/DC CONVERTER

ON	OFF	Control Switch	Sync. Rectifier (SR)	Operating Modes
SES1, SES2	***S***	***Q3, Q4***	***Q1, Q2***	**Low-voltage dual-source-powering mode**
SES1, SES2	***S***	***Q1, Q2***	***Q3, Q4***	**High-voltage dc-bus energy-regenerating mode**
SES1, SES2	***Q1, Q2, Q4***	***S***	***Q3***	**Low-voltage dual-source buck mode**
SES1, SES2	***Q1, Q2, Q4***	***Q3***	***S***	**Low-voltage dual-source boost mode**
-	***SES1, SES2 Q1, Q2, Q3, Q4***	-	-	**System shutdown**

III. STEADY-STATE ANALYSIS

In this section, we analyze the voltage gain, switch voltage stress, and uniform average current sharing characteristics of the proposed BDC when operating in a steady state.

A. Voltage Gain: The voltage gains of the proposed BDC can be derived by applying the principle of inductor volt-second balance to the different modes. To enhance simplicity and practicality, the equivalent series resistances (ESRs) of the inductors L1 and L2 have been substituted into the state equations as non-ideal cases, and the parameters $R_{L1}=R_{L2}=R_L=50m\Omega$ are also given.

1) Low-Voltage Dual-Source-Powering Mode

The relationship among the voltage gains of the three dc sources under steady-state operation are given by;

$$\frac{V_H}{V_{s2}} = \frac{k+1}{1-D_u}$$

$$\frac{V_H}{V_{s1}} = \frac{k}{(1-D_u)(k+1)}$$

Where k is the ratio of $V_{s1}=V_{ES1}$ to $V_{s2}=V_{ES2}$, and D_u is the duty cycle of Q_3 and Q_4 and is >50%.

Accordingly, the relation between dc-bus voltage V_H and the dual-source voltages (V_{ES1}, V_{ES2}) is given by;

$$\frac{V_H}{V_{s1}+V_{s2}} = \frac{1}{1-D_u}; V_{s1} = kV_{s2}$$

2) High-Voltage DC-Bus Energy-Regenerating Mode
Under steady-state operation, the relationship among the voltage gains of the three DC sources is given by;

$$\frac{V_H}{V_{s1}+V_{s2}}=\frac{1}{1-D_u};V_{s1}=kV_{s2}$$

$$\frac{V_{s1}}{V_H}=\frac{D_d k}{k+1}$$
$$\frac{V_{s2}}{V_H}=\frac{D_d}{k+1}$$

Accordingly, the relation between the dual-source voltages (V_{ES1}, V_{ES2}) and the dc-bus voltage V_H is given by;

$$\frac{V_{s1}+V_{s2}}{V_H}=D_d;V_{s1}=kV_{s2}$$

Although these voltage gains are reduced by the ESR of the inductors under the non-ideal situation, the parasitic effect is relatively small and thus the reduced voltage gain can be easily compensated for by increasing the duty control.

3) Low-Voltage Dual-Source Buck/Boost Mode
The relation between the two low-side voltages

$$V_{Es2}-V_{RL2}=D_sV_{ES1};(Buck\ mode)$$
$$V_{ES1}=\frac{1}{1-D}(V_{Es2}-V_{RL2});(Boost\ mode)$$

Where, Ds is the duty cycle of S for the energy transferred from the main energy storage to the auxiliary energy storage, whereas D is the duty cycle of Q3for the energy transferred from the auxiliary energy storage to the main energy storage. The relationship between the two low-side voltages without the effect of the ESR of inductors can be expressed as;

$$V_{Es2}=D_sV_{ES1};(Buck\ mode)$$
$$V_{ES1}=\frac{V_{Es2}}{1-D};(Boost\ mode)$$

B. Charge-Pump Voltage
The voltage across the CB under different modes can be derived as follows.

1) Low-Voltage Dual-Source-Powering Mode

$$V_{ES1}D_u+(V_{ES1}-V_{CB})(1-D_u)=0$$
$$V_{CB}=\frac{V_{ES1}}{(1-D_u)}$$

2) High-Voltage DC-Bus Energy-Regenerating Mode

$$V_{ES1}(1-D_d)+(V_{ES1}-V_{ES2})D_d=0$$
$$V_{CB}=\frac{V_{ES1}}{D_d}$$

C. Voltage Stresses on Switches: To simplify the voltage stress analyses of the converter, the voltage ripples on the capacitors were ignored. The maximum voltage stresses of the main power MOSFETs Q1~Q4 can be obtained directly as;

$$V_{Q1,max}=V_H$$
$$V_{Q2,max}=V_H-V_{CB}$$
$$V_{Q3,max}=V_H-V_{CB}$$
$$V_{Q4,max}=2V_{ES1}-V_{CB}$$

D. Characteristic of Uniform Average Current Sharing

Through charge balance principles and the state-space averaging technique, the averaged state equations can be obtained directly as;

$$\frac{2(i_{l1}-i_{l2})\,(1-D_u)}{C_Bf_{SW}}=0$$
$$\frac{2(i_{l1}-i_{l2})D_d}{C_Bf_{SW}}=0$$
$$\frac{(i_{l1}+i_{l2})R_H-V_H}{R_HC_H}=0$$

Where $I_H=V^*C_H/R_H$.
Also;

$$i_{l1}=i_{l2}=\frac{i_H}{2}$$

From above equation, the uniform average current sharing can be determined, independent of the values of the capacitors.

IV. CONVERTER CONTROL

The converter control structure is as shown in figure 3, which consists of a vehicular strategic management level and the proposed BDC controller. The corresponding realized DSP flowchart for selecting operating modes of the proposed BDC is also shown in fig.4 for reference.
The strategic management level involves electrical power demand estimation and contains a vehicular power and voltage management unit. The global results of the management must maximize the use of the source that best suits the power train power demand, fulfilling the driver and route requirements [21, 25-33]. In FCV/HEV power systems (Fig. 1), the dc-bus voltage of the driving inverter is regulated and powered by the FC stack through a dc-dc converter. Hence, instead of controlling the converter output voltage of each operation mode, the inductor current iL1or iL2 is

detected and compared with the reference current to control the power flow.

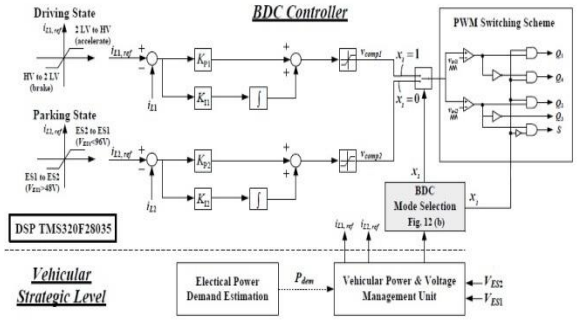

Fig.3: Closed-loop control Scheme [10]

In the converter control structure, the vehicular energy and power and voltage management unit selects the BDC mode according to the operating conditions of the vehicle, such as power demand of different driving state (P_{dem}) and the dual-source voltages (VES1, VES2).It then selects the appropriate current references iL1, for iL2, that can control the active switches (S, Q1~Q4) with proportional integral (PI) or more advanced methods.

Notably, in spite of it is not easy to choose the optimal parameter of PI controller, the advantages of zero steady-state error and capability of noise filtering, making PI control the most widely used industry algorithm. Furthermore, referring to Table I, two switch selector (x1, x2) of BDC controller can be defined for various operating modes. The pulsed-width-modulation (PWM) switching scheme converts the duty cycle determined by different switch selector statuses into gate control signals for the power switches.

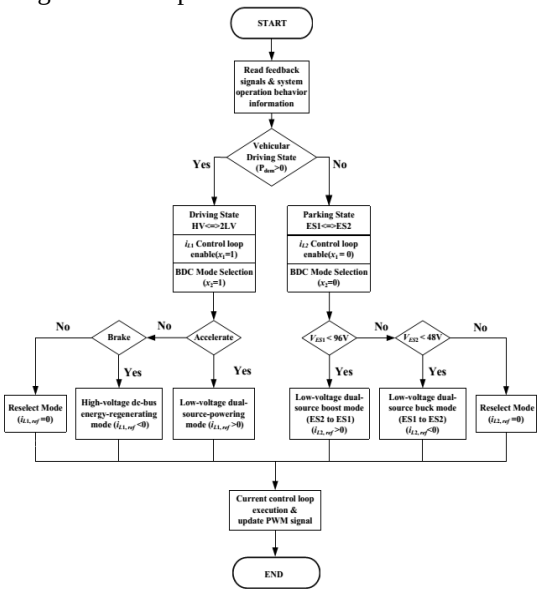

Fig.4: Flowchart for various operating modes of the proposed BDC[10]

The current reference $i_{L1,ref}$ is used to control the bidirectional power flow between the low-voltage dual-source and the high-voltage dc-bus (i.e., 2 LV to HV or HV to 2 LV). In either case, the average inductor current iL2 is equal to the controlled average inductor current iL1 because of the inherent uniform average current sharing in the proposed BDC topology. By contrast, the current reference $i_{L2,ref}$ is used to control the power flow between the main energy storage and the auxiliary energy storage (i.e., ES1 to ES2 or ES2 to ES1).

The procedure of mode switching is shown in Fig. 4. To design the closed-loop controller and simplify the mathematics of the proposed BDC, the MATLAB circuit model is built under the following three assumptions: 1) power switches and diodes are ideal; 2) equivalent series resistances of all inductors and capacitors of the converter are considered to obtain a relatively precise dynamic model; and 3) the converter is operated under a continuous conduction mode.

In the MATLAB circuit model, the adopted circuit parameters are L1=L2=250 μH, CB=10 μF, CH =1880 μF, CES1=CES2=400 μF, the ESR of inductances RL1=RL2=RL=50 mΩ and ESR of capacitances RCB=20 mΩ, RES1=RES2=50 mΩ, and line resistances RES1=12 mΩ and RES2=6 mΩ.

IV. SIMULATION RESULTS AND DISCUSSION

Simulations were conducted to verify the performance of the proposed model for low voltage dual source powering mode as shown in figure 5.

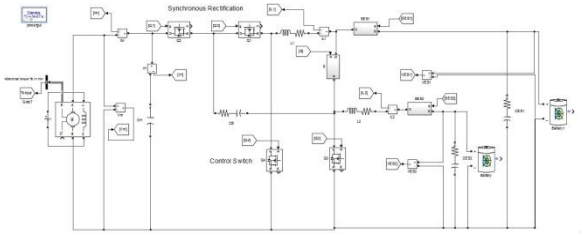

Fig.5: Simulation model for Low Voltage Dual Source Powering mode of Bidirectional Converter

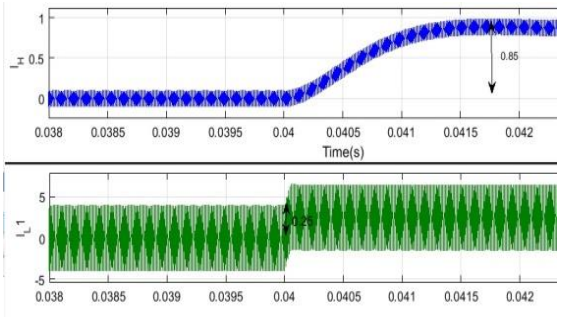

Fig.6: Controlled current step change in the low-voltage dual-source-powering mode: by simulation

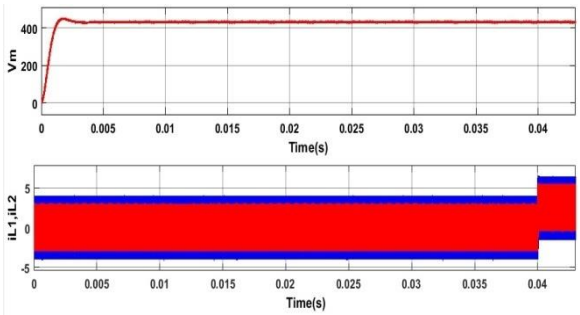

Fig.7: (a) Output voltage at HEV node in the low-voltage dual-source-powering mode (b) Variation of Inductor currents IL1, IL2

The system developed in this study included two loads for the for the low-voltage dual-source-powering mode. The waveform as shown in fig.6 represents that the current I_H has a considerable increase in its value by 0.85A as well as current through inductor L1 increases by 0.25A with the operating mode of bidirectional converter.

V. CONCLUSION

A new BDC topology was proposed to interface dual battery energy sources and high-voltage dc bus of different voltage levels. The circuit configuration, operation principles, analyses, and static voltage gains of the proposed BDC were discussed on the basis of different modes of power transfer. Simulation waveforms highlighted the performance and feasibility of this proposed BDC topology. The highest conversion efficiencies were 95.32% for low-voltage dual-source-powering mode. The results demonstrate that the proposed BDC can be successfully applied in FC/HEV systems to produce hybrid power architecture (has been patented [10]).

VI. REFERENCES

[1]. M. Ehsani, K. M. Rahman, and H. A. Toliyat, "Propulsion system design of electric and hybrid vehicles," IEEE Transactions on industrial electronics, vol. 44, no. 1, pp. 19-27, 1997.

[2]. A. Emadi, K. Rajashekara, S. S. Williamson, and S. M. Lukic, "Topological overview of hybrid electric and fuel cell vehicular power system architectures and configurations," IEEE Transactions on Vehicular Technology, vol. 54, no. 3, pp. 763-770, 2005.

[3]. A. Emadi, S. S. Williamson, and A. Khaligh, "Power electronics intensive solutions for advanced electric, hybrid electric, and fuel cell vehicular power systems," IEEE Transactions on Power Electronics, vol. 21, no. 3, pp. 567-577, 2006.

[4]. E. Schaltz, A. Khaligh, and P. O. Rasmussen, "Influence of battery/ultracapacitor energy-storage sizing on battery lifetime in a fuel cell hybrid electric vehicle," IEEE Transactions on Vehicular Technology, vol. 58, no. 8, pp. 3882-3891, 2009.

[5]. P. Thounthong, V. Chunkag, P. Sethakul, B. Davat, and M. Hinaje, "Comparative study of fuel-cell vehicle hybridization with battery or supercapacitor storage device," IEEE transactions on vehicular technology, vol. 58, no. 8, pp. 3892-3904, 2009.

[6]. C. C. Chan, A. Bouscayrol, and K. Chen, "Electric, hybrid, and fuel-cell vehicles: Architectures and modeling," IEEE transactions on vehicular technology, vol. 59, no. 2, pp. 589-598, 2010.

[7]. A. Khaligh and Z. Li, "Battery, ultracapacitor, fuel cell, and hybrid energy storage systems for electric, hybrid electric, fuel cell, and plug-in hybrid electric vehicles: State of the art," IEEE transactions on Vehicular Technology, vol. 59, no. 6, pp. 2806-2814, 2010.

[8]. K. Rajashekara, "Present status and future trends in electric vehicle propulsion technologies," IEEE Journal of Emerging and Selected Topics in Power Electronics, vol. 1, no. 1, pp. 3-10, 2013.

[9]. C.-M. Lai, Y.-C. Lin, and D. Lee, "Study and implementation of a two-phase interleaved bidirectional DC/DC converter for vehicle and dc-microgrid systems," Energies, vol. 8, no. 9, pp. 9969-9991, 2015.

[10]. C.-M. Lai, "Development of a novel bidirectional DC/DC converter topology with high voltage conversion ratio for electric vehicles and DC-microgrids," Energies, vol. 9, no. 6, p. 410, 2016.

[11]. J. Moreno, M. E. Ortúzar, and J. W. Dixon, "Energy-management system for a hybrid electric vehicle, using ultracapacitors and neural networks," IEEE transactions on Industrial Electronics, vol. 53, no. 2, pp. 614-623, 2006.

[12]. J. Bauman and M. Kazerani, "A comparative study of fuel-cell–battery, fuel-cell–ultracapacitor, and fuel-cell–battery–ultracapacitor vehicles," IEEE Transactions on Vehicular Technology, vol. 57, no. 2, pp. 760-769, 2008.

[13]. M. Ehsani, Y. Gao, and A. Emadi, Modern electric, hybrid electric, and fuel cell vehicles: fundamentals, theory, and design . CRC press, 2009.

[14]. Z. Haihua and A. M. Khambadkone, "Hybrid modulation for dual active bridge bi-directional converter with extended power range for ultracapacitor application," in Industry Applications Society Annual Meeting, 2008. IAS'08. IEEE, 2008, pp. 1-8: IEEE.

[15]. H. Tao, J. L. Duarte, and M. A. Hendrix, "Three-port triple-half-bridge bidirectional converter with zero-voltage switching," IEEE transactions on power electronics, vol. 23, no. 2, pp. 782-792, 2008.

[16]. T. Bhattacharya, V. S. Giri, K. Mathew, and L. Umanand, "Multiphase bidirectional flyback converter topology for hybrid electric vehicles," IEEE Transactions on Industrial Electronics, vol. 56, no. 1, pp. 78-84, 2009.

[17]. H. Krishnaswami and N. Mohan, "Three-port series-resonant DC–DC converter to interface renewable energy sources with bidirectional load and energy storage ports," IEEE Transactions on Power Electronics, vol. 24, no. 10, pp. 2289-2297, 2009.

[18]. Y.-C. Liu and Y.-M. Chen, "A systematic approach to synthesizing multi-input DC–DC converters," IEEE Transactions on Power Electronics, vol. 24, no. 1, pp. 116-127, 2009.

[19]. K. Gummi and M. Ferdowsi, "Double-input dc–dc power electronic converters for electric-drive vehicles—Topology exploration and synthesis using a single-pole triple-throw

switch," IEEE Transactions on Industrial Electronics, vol. 57, no. 2, pp. 617-623, 2010.

[20]. B. Zhao, Q. Song, and W. Liu, "Power characterization of isolated bidirectional dual-active-bridge DC–DC converter with dual-phase-shift control," IEEE Transactions on Power Electronics, vol. 27, no. 9, pp. 4172-4176, 2012.

[21]. L. Jiang, C. C. Mi, S. Li, M. Zhang, X. Zhang, and C. Yin, "A novel soft-switching bidirectional DC–DC converter with coupled inductors," IEEE Transactions on Industry Applications, vol. 49, no. 6, pp. 2730-2740, 2013.

[22]. D.-Y. Jung, S.-H. Hwang, Y.-H. Ji, J.-H. Lee, Y.-C. Jung, and C.-Y. Won, "Soft-switching bidirectional DC/DC converter with a LC series resonant circuit," IEEE Transactions on Power Electronics, vol. 28, no. 4, pp. 1680-1690, 2013.

[23]. H. Wu, K. Sun, S. Ding, and Y. Xing, "Topology derivation of non-isolated three-port DC–DC converters from DIC and DOC," IEEE Transactions on Power Electronics, vol. 28, no. 7, pp. 3297-3307, 2013.

[24]. B. Farhangi and H. A. Toliyat, "Modeling and analyzing multiport isolation transformer capacitive components for onboard vehicular power conditioners," IEEE Transactions on Industrial Electronics, vol. 62, no. 5, pp. 3134-3142, 2015.

[25]. A. Hintz, U. R. Prasanna, and K. Rajashekara, "Novel modular multiple-input bidirectional DC–DC power converter (MIPC) for HEV/FCV application," IEEE Transactions on Industrial Electronics, vol. 62, no. 5, pp. 3163-3172, 2015.

[26]. A. Nahavandi, M. T. Hagh, M. B. B. Sharifian, and S. Danyali, "A non-isolated multiinput multioutput DC–DC boost converter for electric vehicle applications," IEEE Transactions On Power Electronics, vol. 30, no. 4, pp. 1818-1835, 2015.

[27]. C.-M. Lai and M.-J. Yang, "A high-gain three-port power converter with fuel cell, battery sources and stacked output for hybrid electric vehicles and DC-microgrids," Energies, vol. 9, no. 3, p. 180, 2016.

[28]. Y. Jang and M. M. Jovanovic, "Interleaved boost converter with intrinsic voltage-doubler characteristic for universal-line PFC front end," IEEE Transactions on Power Electronics, vol. 22, no. 4, pp. 1394-1401, 2007.

Pacific (ITEC Asia-Pacific), 2016 IEEE Conference and Expo, 2016, pp. 163-166: IEEE.